

# Numerical Analysis of the Dynamic Two-Phase Flow Behavior in the Ionic Compressor with a Novel H-shaped Piston



Zekun Liu, Xiang Kang, and Yun Li

**Abstract** With the development of the hydrogen energy industry, it is crucial for hydrogen refueling stations that compressors can work efficiently and flexibly with a longer life span. Adopting ionic liquid as a liquid piston to compress hydrogen is a feasible method. The high stroke frequency of ionic compressor prevents the liquid piston from maintaining a stable shape, leading to the generation of the additional clearance volume and hydrogen sealing failure. In this article, a novel H-shaped piston was proposed and a 3D numerical model of an ionic compressor cylinder with it was established. The dynamic simulation of the two-phase fluid behavior in the cylinder during three cycles was performed using the volume of fluid method and the dynamic mesh technique. The effect of this piston on the variation of the two-phase interface and the clearance volume of the compressor has been discussed for optimizing the design of the ionic compressor. Results show that: the clearance volume of the cylinder with a H-shaped piston was smaller than that of the cylinder with a normal piston in all three compression cycles, which indicated that the higher volumetric efficiency could be obtained with the H-shaped piston. In addition, the application of the H-shaped piston allowed sufficient ionic fluid to be retained in critical sealing locations of the cylinder to keep hydrogen sealing and piston lubrication well.

**Keywords** Ionic compressor · H-shaped piston · Clearance volume

## 1 Introduction

As pollution-free and sustainable green energy, hydrogen has received increasing attention in the energy industry over the past few years. Hydrogen fuel cell electric vehicles (HFCEV) is an essential part of hydrogen energy industry. The popularization of HFCEVs is limited by the driving mileage, which depends

---

Z. Liu · X. Kang · Y. Li (✉)  
Xi'an Jiaotong University, Xi'an, China  
e-mail: [yunli@xjtu.edu.cn](mailto:yunli@xjtu.edu.cn)

© The Author(s), under exclusive license to Springer Nature Switzerland AG 2024  
M. Read et al. (eds.), *13th International Conference on Compressors and Their Systems*,  
Springer Proceedings in Energy, [https://doi.org/10.1007/978-3-031-42663-6\\_31](https://doi.org/10.1007/978-3-031-42663-6_31)

383

on the hydrogen filling pressure. Thus, efficient, high-pressure, stable and high-displacement hydrogen pressurization equipment is crucial to the advancement of the HFCEV industry. Hydrogen compressor is one of the most important equipment in a hydrogen refueling station, the cost of which usually accounts for more than 30% of the total construction cost of a hydrogen refueling station [1]. The development of high-pressure hydrogen compressors can promote the popularity of hydrogen refueling facilities significantly.

Ionic compressor is a novel compressor that utilizes ionic liquid as a liquid piston to compress hydrogen gas. Ionic liquids can offer good thermal stability, low compressibility, suitable viscosity, and excellent frictional properties. They have low solubility with hydrogen gas so that hydrogen gas can't be contaminate. Benefiting from the excellent physicochemical properties of ionic liquids, ionic liquids can be used in ionic compressors for both sealing and lubrication functions, solving the problem of hydrogen sealing and oil-free lubrication at high pressure in piston compressors.

Ionic compressor is a kind of liquid piston compressor in terms of working principle. Van de Ven et al. [2] developed several heat transfer models for liquid piston compressors corresponding to different applications and demonstrate by CFD methods that liquid pistons would effectively improve the heat transfer efficiency in the cylinder of compressors and lead the compression process closer to isothermal compression. Saadat et al. [3] obtained the optimal compression/expansion profile for a specific geometry of cylinder in a liquid piston air compressor by numerical methods, and demonstrated the effectiveness of the optimal profile to improve the compression efficiency. Patil et al. [4, 5] proposed various methods to improve the heat transfer efficiency of liquid piston compressors, including the application of porous media, optimized cylinder profile, in-cylinder spray, and investigated the ability of these methods to improve the compression efficiency experimentally. Kermani [6] presented a numerical model for the heat transfer process in an ionic compressor and devised an experimental prototype of a single-stage low-speed ionic compressor. Guo et al. [7] established a two-dimensional cylinder model of an ionic compressor and simulated the two-phase behavior in a single cycle to investigate the effects of liquid viscosity on the turbulent kinetic energy in the ionic compressor cylinder.

To meet the demand for large compressor displacements in commercial hydrogen refueling stations with the limited reciprocating volume of compressors, ionic compressors have a stroke frequency as fast as 5.8 Hz, while liquid piston compressors for air storage have a stroke frequency of only 0.2–0.5 Hz. High speed reciprocating motion leads to deformation of the liquid piston. During the movement of the liquid piston, droplets and bubbles continuously generate and break up in the cylinder due to the interaction between the ionic liquid and the hydrogen gas, which could hinder the normal discharge of hydrogen gas in the discharge process. The hydrogen gas trapped in the cylinder prolongs the expansion process of the compressor and increases the clearance volume of the cylinder, leading to a reduction in compressor efficiency. In addition, there should be enough ionic liquid in the critical sealing part of the cylinder such as the contact surface between the solid piston and the cylinder

wall for sealing and lubrication during the compressor operation. Nevertheless, it has been found by CFD simulations that when the piston moves to the bottom dead center, it often fails to maintain a complete liquid film on the piston surface, which could lead to the failure of the compressor sealing and lubrication.

In this article, a numerical model of the ionic compressor cylinder with a novel H-shaped piston was established. 3D dynamic simulations were performed to obtain the behavior of the gas–liquid two-phase flow in the cylinder during multiple compression cycles by means of the dynamic grid technique and the volume of fluid (VOF) method. The variation of the two-phase interface and the compressor clearance volume was analyzed to demonstrate the positive influence of the H-piston on the compressor sealing process and volumetric efficiency.

## 2 Methodology

### 2.1 Physical Model

The ionic compressor for hydrogen refueling station normally consists of five stages with minimum suction pressure of 0.5 MPa and maximum discharge pressure of 90 MPa. The first stage of a five-stage ionic compressor was studied in this article. The simplified model is shown in Fig. 1, and the basic design parameters of cylinder are shown in Table 1.

The diameter  $D_j$  of the cylinder and the piston stroke  $S$  are given by Eqs. (1) and (2), respectively.

$$D_j = \sqrt{\frac{4V_s}{\pi S}} \tag{1}$$

Fig. 1 Simplified physical model

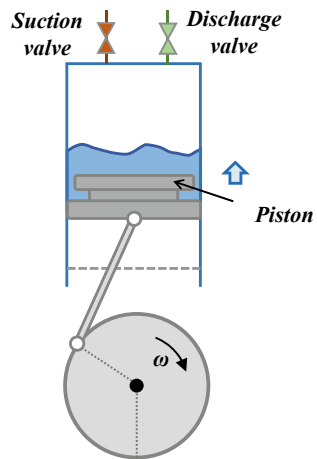


**Table 1** Design parameters of the cylinder

Parameters	Suction pressure (MPa)	Discharge pressure (MPa)	Volume flow rate of hydrogen gas (Nm <sup>3</sup> /h)
Value	0.5	1.4	370
Parameters	Stroke frequency (Hz)	Gas temperature in suction valve (K)	Relative clearance volume (%)
Value	5.8	300	5

$$S = \frac{30C_m}{n} \tag{2}$$

where  $C_m$  is the average velocity of piston (m/s),  $n$  is the rotation speed of the compressor (rpm),  $V_s$  is the stroke volume of compressor (m<sup>3</sup>), which is given by Eq. (3).

$$V_s = \frac{q_v}{\eta v n} \tag{3}$$

where  $q_v$  is the volumetric flow rate of the compressor (m<sup>3</sup>/min),  $\eta v$  is the discharge coefficient.

The displacement of the solid piston  $x$  can be obtained from Eq. (4).

$$x = r \left[ (1 - \cos \theta) - \frac{1}{\lambda} (1 - \sqrt{1 - \lambda^2 \sin^2 \theta}) \right] \tag{4}$$

where  $r$  is crank radius,  $l$  is the length of the connecting rod,  $\lambda$  is the ratio of the crank radius to the length of the connecting rod,  $\theta$  is the crank angle, and the curve of the piston displacement is shown in Fig. 2.

**Fig. 2** Piston displacement

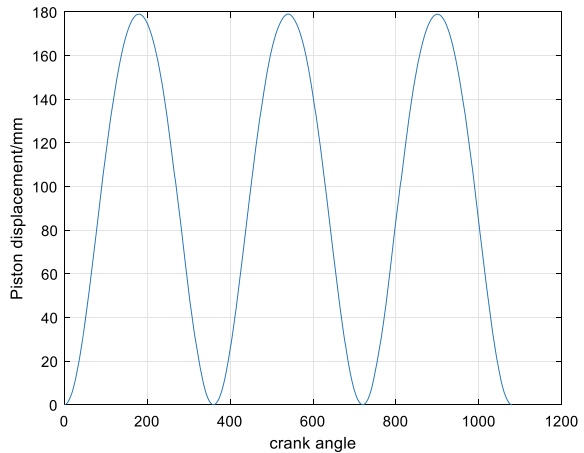


**Table 2** Geometric parameters of the physical model

Parameters	Value
Diameter of the cylinder (mm)	180
Stroke of the piston movement (mm)	179
Height of the liquid layer in the cylinder (mm)	38
Effective diameter of both suction and discharge valves (mm)	40
Crank radius (mm)	89.5
Connecting rod length (mm)	400

**Table 3** Geometric parameters of the physical model (298.15 K)

Property	Density (kg/m <sup>3</sup> )	Heat capacity (J/mol K)
Valve	1436.8	524
Property	Thermal conductivity (W/m K)	Dynamic viscosity (mPa s)
Valve	0.128	50.8

The geometry parameters of cylinder model can be calculated, as shown in Table 2. The physical parameters of the ionic liquid employed in this research are shown in Table 3.

## 2.2 Numerical Model and Solution Method

The main challenge in simulating two-phase behavior in a compressor cylinder is to capture the two-phase interface accurately. The VOF method is an excellent way for dealing with two-phase flow problems. Two or three immiscible fluids can be simulated by the VOF method through tracking the volume fraction of each phase in each grid and solving a single momentum equation. The VOF method has been reported to be one of the most powerful tools to deal with stratified compressible two-phase flows. Thus, this research used the VOF model to calculate the complex two-phase flow in the cylinder during the operation of the ionic compressor.

The control equations were discretized in the Fluent software [8] by the finite volume method (FVM). The  $k-\omega$  SST turbulence model was applied to calculate the turbulence flow. The convective term, turbulent kinetic energy and specific dissipation rate were discretized with the second order upwind format. Further, the pressure staggering option (PRESTO) method was adapted to interpolate the pressure gradient of the source term in the momentum equation. The upper surface of the solid piston is a moving boundary. The motion of the moving boundary is controlled by the UDF through the dynamic mesh technique. The boundary conditions of the inlet and the outlet are shown in Eqs. (5) and (6), respectively.

$$\begin{cases} \text{Wall, } p \geq 0.5 \text{ MPa} \\ \text{Pressure inlet}(0.5 \text{ MPa}), p < 0.5 \text{ MPa} \end{cases} \quad (5)$$

$$\begin{cases} \text{Wall, } p \leq 1.4 \text{ MPa} \\ \text{Pressure outlet}(0.5 \text{ MPa}), p > 1.4 \text{ MPa} \end{cases} \quad (6)$$

The basic assumptions in the numerical model are as follows.

(1) The ionic liquid is considered as incompressible fluid. (2) There is no mass transfer between hydrogen and ionic liquid. (3) No phase change occurs for both ionic liquid and hydrogen gas during the compressor operation process. (4) Cylinder walls are adiabatic and no relative sliding occurs between the fluid and the walls.

The moving mesh was realized by the laying method, which requires all grids in the model to be structural grid. Thus, the mesh type was determined as hexahedral type mesh. After verification of grid independence, the total number of grids is determined to be one million.

### 3 Results and Discussions

Figures 3, 5 and 7 show the phase fields in cylinder during the first three compression cycles, demonstrating the variation of the two-phase interface. The red area in the phase field represents hydrogen gas, the blue area is filled with ionic liquid, and the green area refers to the interface of two phases. The velocity field in the cylinder of the ionic compressor during the first three cycles is presented in Figs. 4, 6 and 7. The single reciprocating cycle lasts 0.2 s. The first half cycle is the compression and discharge process followed by the expansion and suction process in the second half cycle. The initial ionic liquid height is 5 mm, above the top surface of the H-shaped piston.

It can be seen in Figs. 3 and 4, the shape of the liquid piston remained stable and no gas vortices were generated in the cylinder during compression and discharge process of the first cycle. When the liquid piston contacted the top surface of the cylinder, a part of the ionic liquid was discharged through the outlet along with the gas, when the piston was close to the top dead center. Several bubbles appeared in the liquid piston near the left cylinder wall, due to the viscous effect between the ionic liquid and the cylinder wall, as shown in the phase field at the time of 0.1 s. As shown in Fig. 4, the fluid flow rate in the cylinder is as low as 1.8 m/s during the expansion process from 0.1 to 0.1039 s. The hydrogen gas flowed into the cylinder with a maximum velocity of 39.6 m/s during the suction process from 0.1029 to 0.2 s, when the liquid was moving at a low speed because of the viscous effect with the cylinder wall, and there was an obvious separation between the liquid piston and the solid piston. As shown in Fig. 4, two small vortexes were observed on the either side of the intake gas flow at the time of 0.1375 s, the sizes of which increased during the movement of the solid piston to the bottom dead center. As a result of the interaction

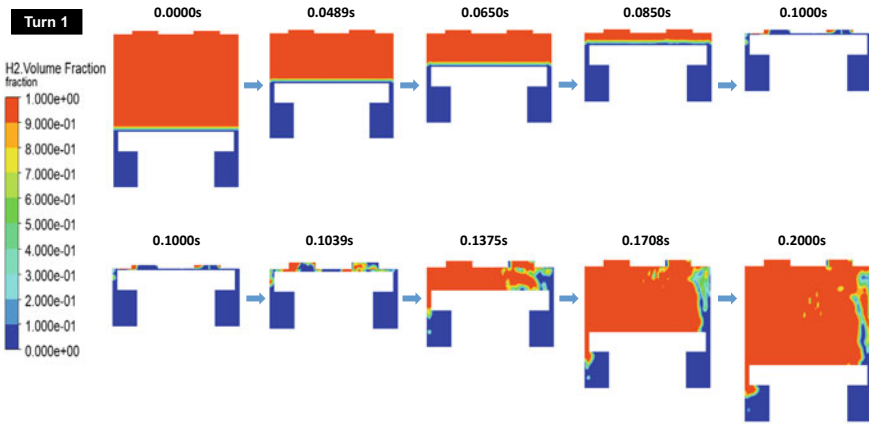


Fig. 3 Phase field in the cylinder during the first compression cycle

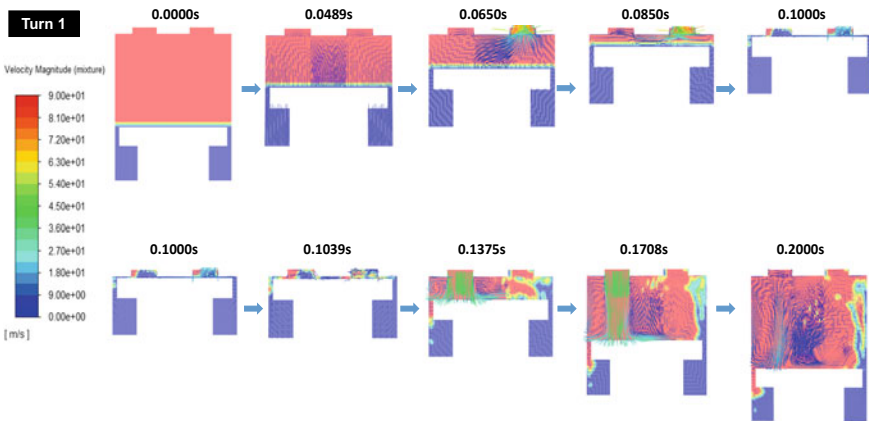


Fig. 4 Velocity field in the cylinder during the first compression cycle

between the gas vortex and the liquid, part of the liquid adhered to the right cylinder wall in the form of a liquid film, part of the liquid transformed into small droplets and moved towards the liquid film, and a small part of the gas enters the ring gap of the H-shaped piston to generate bubbles. The distribution and movement trend of the liquid in the cylinder conforms to the distribution of the vortex in the cylinder, as shown in Fig. 4.

The transition of the interface between two phases during the second compression cycle is presented in Figs. 5 and 6. The gas vortices developed during the suction process of the previous cycle was still existing in the cylinder throughout the compression process from 0.2 to 0.2504 s and gradually disappeared after the start of the discharge process, as shown in Fig. 6. It can be found in Fig. 5 that the liquid on the right side of the cylinder wall accompanying with part of the gas quickly went

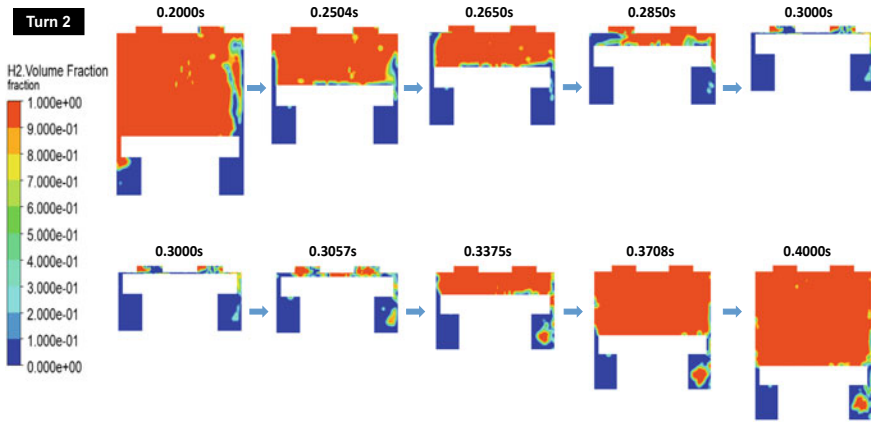


Fig. 5 Phase field in the cylinder during the second compression cycle

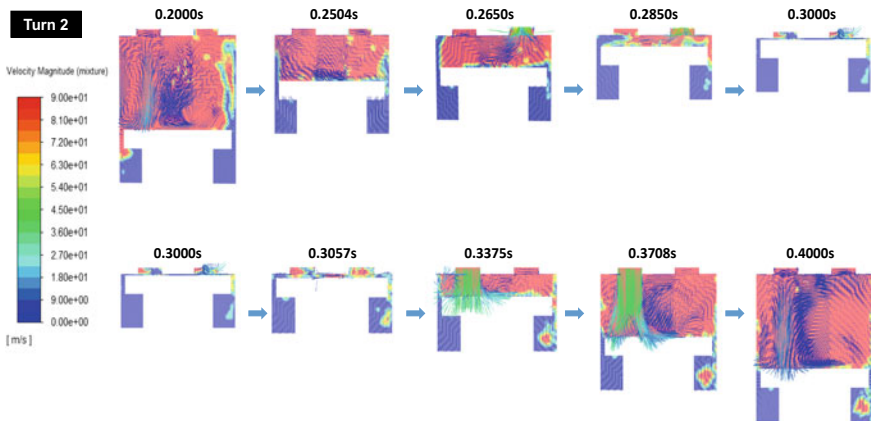
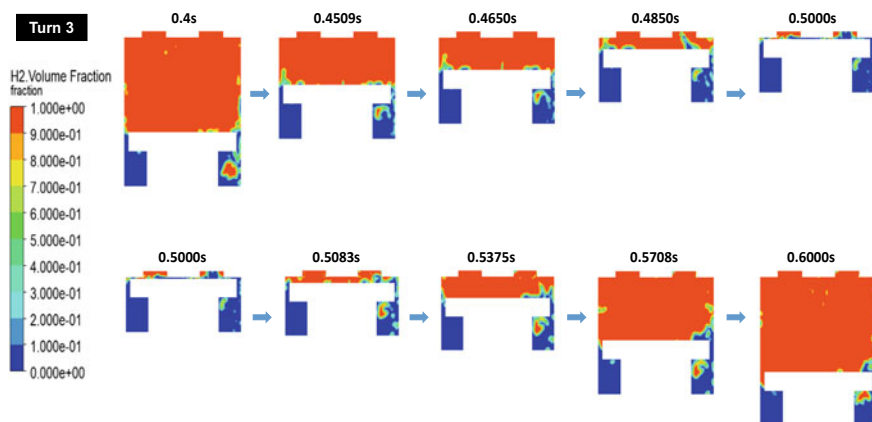


Fig. 6 Velocity field in the cylinder during the second compression cycle

back to the ring gap of the H-shaped piston, and the liquid in the left side of ring gap moved quickly upward along the cylinder wall pushed by the solid piston during the movement of the solid piston to the top dead center. There was no bubble in the left side of ring gap while several bubbles existed in the right side of ring gap at the end of discharge process as shown in phase field at 0.3 s. During the movement of the solid piston to the bottom dead center, sufficient ionic liquid was still observed in the sealing position between the piston and the cylinder wall to perform the sealing and lubricating function, although a large amount of gas entered ring gap due to the difference in velocity of the liquid movement and the solid piston movement. As shown in the Fig. 6, two gas vortices were found on the either side of the intake gas flow at the time of 0.3375 s, when the maximum velocity of 47.3 m/s during the suction process was obtained. During the movement of the piston to the bottom dead





**Fig. 7** Phase field in the cylinder during the third compression cycle

center, the size of the right vortex kept increasing, while the left vortex splits into two small vortices with the restriction of the liquid on the cylinder wall.

The transition of the interface between two phases during the third compression cycle is presented in Figs. 7 and 8. As shown in Fig. 7, part of gas trapped in the ring gap of the H-shaped piston left the ring gap in the process of the piston moving to the top dead center. It can be seen in the phase field at 0.5 s that there was still a small part of gas trapped in the ring gap at the end of the discharge process. As shown in the Fig. 8, two gas vortices were observed on the either side of the intake gas flow at the time of 0.5375 s, sizes of which kept increasing during the suction process from 0.5375 to 0.6 s. The maximum velocity of the two-phase flow was 41.7 m/s in the expansion and the suction process. The vortex on the left side of the cylinder by the action of the liquid on the cylinder wall tended to split into two vortices, but the second vortex did not succeed in forming at the end of the suction, which was different compared to the second cycle. The vortex in the left side of the cylinder tended to split into two small vortices with the restriction of the liquid on the cylinder wall, but the second vortex did not succeed in generation until the end of the suction process, which was different compared to the second cycle.

It can be seen in the velocity field that the ionic liquid in the ring gap of H-shaped piston always maintained a low velocity over multiple compression cycles. Consequently, there was always sufficient ionic fluid at the critical sealing location between the piston and the cylinder, even though some gas would enter the ring gap during the entire compression cycle. The liquid piston cannot maintain a stable shape under the interaction with cylinder walls and gas vortices. Part of the liquid adhered to the cylinder wall to form a liquid film, and part of the liquid was transformed into small droplets dispersing in the cylinder. It was apparent that the distribution of the liquid in the cylinder corresponds to the distribution of the vortices.

As can be found in Figs. 4, 6, and 8, a part of the ionic liquid left the cylinder accompanying with the hydrogen gas during the discharge process of each compression

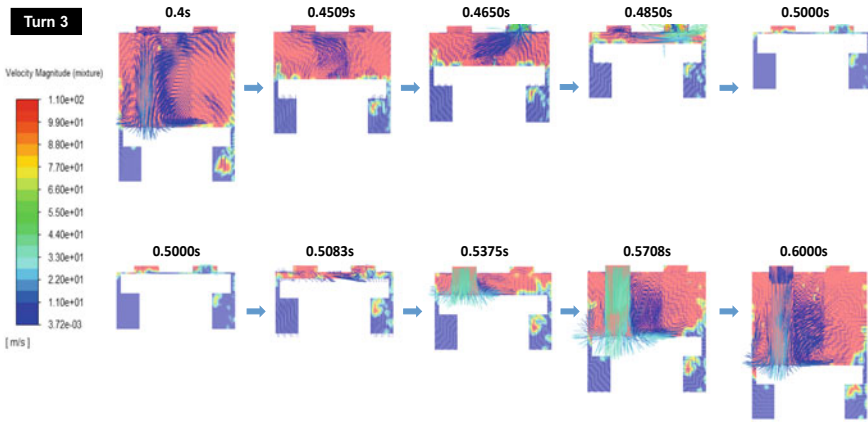
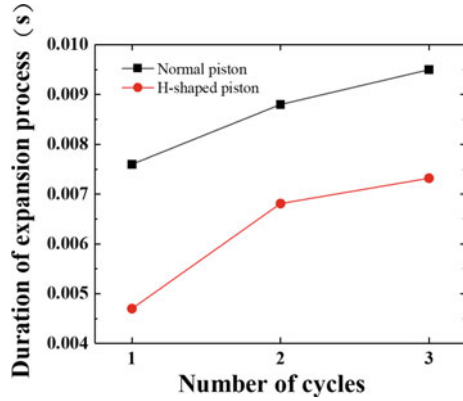


**Fig. 8** Velocity field in the cylinder during the third compression cycle

cycle, while some of the gas was trapped in the cylinder and could not be discharged in time, which caused an increase in the clearance volume of the compressor. The increase in the clearance volume led to a longer expansion process and a reduction in the volumetric efficiency of the compressor. Figure 9 illustrates the duration of the expansion process at different cycles for the case with an H-shaped piston and the case with a normal piston. The duration of the expansion process in the first compression cycle with an H-shaped piston was 0.0047 s, which was much shorter than 0.0076 s for a normal piston cylinder. During the second and third compression cycles, the duration of the expansion process increased in both cases as a result of the continuous loss of ionic liquid, but it was obvious that the duration of the expansion process in the case with a H-shaped piston was always lower than that in the case with normal piston. It is demonstrated that the application of the novel H-shaped piston can effectively reduce the clearance volume and improve the efficiency of the compressor comparing with the normal piston, while the H-shaped piston can keep sufficient ionic liquid in the sealing location between the piston and the cylinder wall to perform the sealing and lubricating functions throughout the compression cycles.

**Fig. 9** Duration of the expansion process at different cycles for the case with an H-shaped piston and the case with a normal piston



### 4 Conclusion

In this article, a numerical model of an ionic compressor cylinder with a novel H-shaped piston has been established, and dynamic 3D simulations has been carried out to investigate the two-phase behavior in the cylinder by the VOF method and the dynamic mesh technique. The effect of the H-shaped piston on the variation of the two-phase interface and the clearance volume of the compressor has been discussed for optimizing the design of the ionic compressor.

Main conclusions of this study can be summarized as follows:

The shape of the liquid piston could not remain stable during all three compression cycles. A part of the ionic liquid leaked out of the cylinder in the discharge process of each compression cycle, resulting in an increase in the clearance volume of the compressor. There was always sufficient ionic liquid retained in the sealing location between the piston and the cylinder wall to perform the sealing and lubrication functions of the compressor.

Two gas vortices were observed and increased in size with the movement of the solid piston in the suction process of all three compression cycles. The vortex in the left side of the cylinder split into two small vortices due to restriction of the liquid on the cylinder wall, which occurred in the late second cycle. It was demonstrated that the distribution of the liquid in the cylinder corresponded to the distribution of the gas vortex.

The clearance volume of the cylinder with an H-shaped piston was smaller than that of the cylinder with a normal piston in all three compression cycles, which indicated that the higher volumetric efficiency of the compressor could be obtained with the H-shaped piston.

## References

1. N.A. Kermani, Evaluation of ionic liquids as replacements for the solid piston in conventional hydrogen reciprocating compressors: a review. *Int. J. Hydrogen Energy* **45**(33), 16337–16354 (2020)
2. J. Ven, Liquid piston gas compression. *Appl. Energy* **86**(10), 2183–2191 (2009)
3. M. Saadat, Optimal trajectories for a liquid piston compressor/expander in a Compressed Air Energy Storage system with consideration of heat transfer and friction, in *American Control Conference (ACC)*, pp. 2725–2730. IEEE, Montreal (2012)
4. V.C. Patil, Experimental investigation of heat transfer in liquid piston compressor. *Appl. Thermal Eng.* **146**, 169–179 (2018)
5. V.C. Patil, Experimental study of heat transfer enhancement in liquid piston compressor using aqueous foam. *Appl. Therm. Eng.* **164**(3), 114441 (2019)
6. N.A. Kermani, *Design and prototyping of an ionic liquid piston compressor as a new generation of compressors for hydrogen refueling stations* (Technical University of Denmark, Copenhagen, Denmark, Doctor, 2017)
7. G. Yi, Numerical analysis of the dynamic two-phase flow behaviour in the ionic liquid compressor for hydrogen refuelling stations. *Appl. Thermal Eng.* **219**, 119607 (2023)
8. A. Flunet, *2020R2* (Ansys Inc., Canonsburg, 2020)